Human Molecular Genetics, 2013, Vol. 22, No. 2 ***313–327***
doi:10.1093/hmg/dds430
Advance Access published on October 16, 2012

Primordial germ cells and gastrointestinal stromal tumors respond distinctly to a cKit overactivating allele

Li Chen, Mehlika Faire, Michael D. Kissner and Diana J. Laird*

Department of Obstetrics/Gynecology and Reproductive Sciences, Eli and Edythe Broad Center for Regeneration Medicine and Stem Cell Research, UCSF, San Francisco, CA 94143-0667, USA

Received August 10, 2012; Revised October 1, 2012; Accepted October 8, 2012

KitL, via its receptor cKit, supports primordial germ cell (PGC) growth, survival, migration and reprogramming to pluripotent embryonic germ cells (EGCs). However, the signaling downstream of KitL and its regulation in PGCs remain unclear. A constitutively activating mutation, *cKit*$^{V558\Delta}$, causes gain-of-function phenotypes in mast cells and intestines, and gastrointestinal stromal tumors (GISTs) when heterozygous. Unexpectedly, we find that PGC growth is not significantly affected in *cKit*$^{V558\Delta}$ heterozygotes, whereas in homozygotes, increased apoptosis and inefficient migration lead to the depletion of PGCs. Through genetic studies, we reveal that this oncogenic *cKit* allele exhibits loss-of-function behavior in PGCs distinct from that in GIST development. Examination of downstream signaling in GISTs from *cKit*$^{V558\Delta/+}$ mice confirmed hyperphosphorylation of AKT and ERK, but both remain unperturbed in *cKit*$^{V558\Delta/+}$ PGCs and EGCs. In contrast, we find reduced activation of ERK1/2 and JNK1 in *cKit*$^{V558\Delta}$ homozygous PGCs and EGCs. Inhibiting JNK, though not ERK1/2, increased apoptosis of wild-type PGCs, but did not further affect the already elevated apoptosis of *cKit*$^{V558\Delta/V558\Delta}$ PGCs. These results demonstrate a cell-context-dependent response to the *cKit*$^{V558\Delta}$ mutation. We propose that AKT overload protection and JNK-mediated survival comprise PGC-specific mechanisms for regulating cKit signaling.

INTRODUCTION

Primordial germ cells (PGCs) are the embryonic founders of the adult gametes. In most animals, PGCs are set aside as a distinct cell lineage during early embryogenesis. Mammalian PGCs are specified from the epiblast at E7.25 in mice and traverse many tissues before eventually colonizing the gonad at E11.5 (1). During their migration, PGCs undergo proliferation, increasing from approximately 100 at E8.5 to approximately 3000 at E11.5 and continue to divide in the genital ridges, where they differentiate along male- or female-specific gametogenesis programs (2). PGCs are also the source of pluripotent stem cells called embryonic germ cells (EGCs) that resemble embryonic stem cells (ESCs) in their properties and gene expression (3,4).

cKit and its ligand (KitL), encoded by *W* and *Steel* loci, respectively, are essential for PGC survival, migration and proliferation in mice. Loss-of-function cKit mutations result in the failure of PGC proliferation after E8.5, impaired migration and a large proportion of ectopic PGCs (5,6). Dynamic regulation of KitL expression in somatic cells promotes the survival of properly localized PGCs and the apoptosis of ectopic PGCs (7,8). *In vitro* culture experiments demonstrate that soluble KitL [or stem cell factor (SCF)] is required in a dose-dependent manner for PGC survival (9), proliferation (10) and migration (11,12). On the other hand, *cKit* gain-of-function mutations are typically oncogenic (13,14). A frequent mutation in the second kinase domain, at Valine 816, is associated with testicular germ cell tumors, but may promote their progression rather than initiation (15–17). Activating mutations in the cKit juxtamembrane (JM) domain are found in human gastrointestinal stromal tumors (GISTs), and a mouse model of the most frequently mutated residue, V558 (V559 in human), replicates the disease (14,18,19); these mutations presumably disrupt JM-mediated inhibition of cKit autophosphorylation in the absence of KitL (20). Tyrosine phosphorylation, accelerated by KitL-induced receptor dimerization, provides docking sites for mediators of several

*To whom correspondence should be addressed. Tel: +1 4154765471; Fax: +1 4155027866; Email: lairdd@stemcell.ucsf.edu

signaling pathways: PI3K/AKT, MAPK, JAK-STAT and Src (21–25). The functions of these respective pathways in PGCs remain largely opaque. The absence of PGC phenotypes in mouse models with deletions of the tyrosine docking residues for PI3K (Tyr719) and Src (Tyr 567/569) present a conundrum for understanding these important pathways in this rare and relatively inaccessible cell type (26–28).

Here, we used an activating mutation, $cKit^{V558\Delta}$, to ascertain the *in vivo* consequences of cKit pathway overstimulation for PGCs. Through genetic and biochemical studies, we found that the $cKit^{V558\Delta}$ mutation does not significantly affect PGC growth in heterozygotes and causes unexpected PGC depletion and loss of MAPK signaling in homozygotes. Our results suggest that the signaling requirements of PGCs are distinct from GISTS and furthermore uncover JNK as an important effector of cKit-mediated PGC survival.

RESULTS

A constitutively activating cKit mutation, *V558Δ*, does not disrupt PGC development in heterozygotes, but causes PGC depletion in homozygotes

To investigate the consequence of cKIT over-activation for PGC development, we examined a mouse mutant with a targeted deletion of Valine 558 ($cKit^{V558\Delta}$), a residue in the JM domain (18). Gain-of-function phenotypes in diverse tissues have been described in $cKit^{V558\Delta}$ heterozygotes: a 4-fold increase in mast cell number, increase in skin melanocytes and 100% penetrant GIST [P. Besmer, personal communication (18)]. In contrast to these phenotypes, testes and ovaries of $cKit^{V558\Delta/+}$ appeared grossly normal in size, weight and morphology, and testicular tumors were not detected in adult mice by the time of their mortality at 3–6 months of age from GISTs ($n = 10$) (Supplementary Material, Fig. S4). In E17.5 $cKit^{V558\Delta/V558\Delta}$ fetal testes, we did not observe any Nanog and E-cadherin-expressing neoplasias (Supplementary Material, Fig. S1A) as has been described on genetic backgrounds conducive to teratomas (29).

Upon examining mid-gestation embryos, we observed an unexpected PGC phenotype. By E11.5, as PGCs aggregate and colonize the gonads, a marked depletion was observed in $cKit^{V558\Delta/V558\Delta}$ by whole-mount immunostaining for the PGC marker GCNA (Fig. 1A). Quantitative image analysis of E11.5 gonads (12) revealed a corresponding decrease in PGCs of homozygotes (mean 371 ± 76 PGCs) compared with WT (1909 ± 549) or $cKit^{V558\Delta/+}$ (1142 ± 270) littermates ($P < 0.05$, Fig. 1B). Although cKIT protein is detectable in PGCs as early as E7.75 (30,31) and *cKit* loss-of-function mutants exhibit measurable PGC loss by E9.0 (5), we did not observe earlier phenotypes in $cKit^{V558\Delta}$ homozygotes. At E8.0–8.5, alkaline phosphatase (AP) staining revealed normal PGC incorporation into the hindgut and comparable PGC numbers between WT and $cKit^{V558\Delta/V558\Delta}$ embryos (Fig. 1C), suggesting that PGC specification occurs normally in these mutants. Interestingly, $cKit^{V558\Delta/+}$ embryos show a slight and transient increase in PGC numbers at E8.0–8.5 (Fig. 1C), whereas no differences in PGC numbers could be detected near the end of PGC migration at E10.5 (Fig. 1A).

The observed deficit of PGCs in $cKit^{V558\Delta/V558\Delta}$ mutants could arise by altered rates of apoptosis, proliferation or migration, and cKit has been implicated in all of these cellular mechanisms (5,9). In E11.5 histologic sections, we found a 3.0-fold increase in the frequency of $SSEA1^{+}$ PGCs expressing the apoptotic marker cPARP in $cKit^{V558\Delta/V558\Delta}$ gonads ($1.74 \pm 0.23\%$) compared with either WT or heterozygotes (0.59 ± 0.17 and $0.69 \pm 0.16\%$, respectively), as shown in Figure 1D. Examining proliferation by 5-ethynyl-2′-deoxyuridine (EdU) incorporation and phospho-histone H3, we observed no significant differences between the three genotypes (Fig. 1E and data not shown). Finally, we quantified the efficiency of PGC migration at E11.5, after the majority of PGCs have colonized the gonads. In serial sections, we observed increased accumulation of PGCs in the dorsal mesentery ($7.99 \pm 3.17\%$ of the total number) of $cKit^{V558\Delta/V558\Delta}$ compared with WT embryos ($1.02 \pm 0.99\%$, Fig. 1F). Taken together, these results indicate that PGC depletion of $cKit^{V558\Delta/V558\Delta}$ embryos is due to increased apoptosis and aberrant migration. In support of this conclusion, we observed in double-mutant analysis that the *V558Δ* phenotype was partially rescued by genetic removal of the pro-apoptotic gene *Bax* (Supplementary Material, Fig. S2); the total number of PGCs in $cKit^{V558\Delta/V558\Delta};Bax^{-/-}$ embryos was increased over $cKit^{V558\Delta/V558\Delta}$ at E11.5. However, the number of ectopic PGCs also increased in double mutants, similar to the previous cross between a null allele for *KitL* and *Bax* (7,32).

We compared the unexpected PGC phenotype of $cKit^{V558\Delta/V558\Delta}$ embryos with that of loss of function alleles of *cKit*. In a genome-wide recessive ethylnitrosourea (ENU) mutagenesis screen for PGC defects, we identified such a novel allele, $cKit^{S830R}$ (33). Sequencing revealed an A → C change at Chr5: 76 048 608 (NCBI37/mm9) that produces a substitution of serine 830 by arginine in the second kinase domain of the predicted protein (Supplementary Material, Fig. S3). $cKit^{S830R/+}$ mice were characterized by white spots on their belly and back (Fig. 3A and Supplementary Material, Fig. S3) similar to the pigment defects in the null allele $cKit^{W}$ (6). Most $cKit^{S830R/S830R}$ mice died perinatally, and the few escapers that survived to adulthood were black-eyed, albino and failed to breed (Supplementary Material, Fig. S3). As early as E8.0 (4–6 somite stages), a deficit in the number of PGCs in $cKit^{S830R/S830R}$ mutants could be detected by AP staining; whereas 50–80 PGCs were present in wild-type, $cKit^{S830R}$ homozygotes possessed ∼20–50 ($P < 0.001$; Fig. 2A). Furthermore, $cKit^{S830R}$ mutant PGCs tended to adhere together in clumps at the base of allantois at this stage, reminiscent of $KitL^{Sl/Sl}$ mutants (32), whereas they have already incorporated into the endoderm pocket in wild-type and $cKit^{S830R/+}$ littermates (data not shown). By the 9–12 somite stage, whereas PGCs in WT embryos increase rapidly (∼90–110), the number in $cKit^{S830R/S830R}$ embryos remained around 40, and did not rise at E10.5 (25 ± 3.2 compared with 816 ± 68 in wild-type) or by E11.5 (6 ± 0.8 compared with 2414 ± 176 in wild-type, Fig. 2B, C and E). PGC depletion in these mutants is at least partially due to excessive apoptosis, as the loss of one Bax allele slightly increased $cKit^{S830R/S830R}$ PGC number to 45.5 ± 5.3 ($P < 0.001$) and the loss of two Bax alleles significantly increased $cKit^{S830R/S830R}$ PGC number from 10 ± 3.9 to 130 ± 6.4 at E10.5 ($P < 0.001$; Fig. 2D).

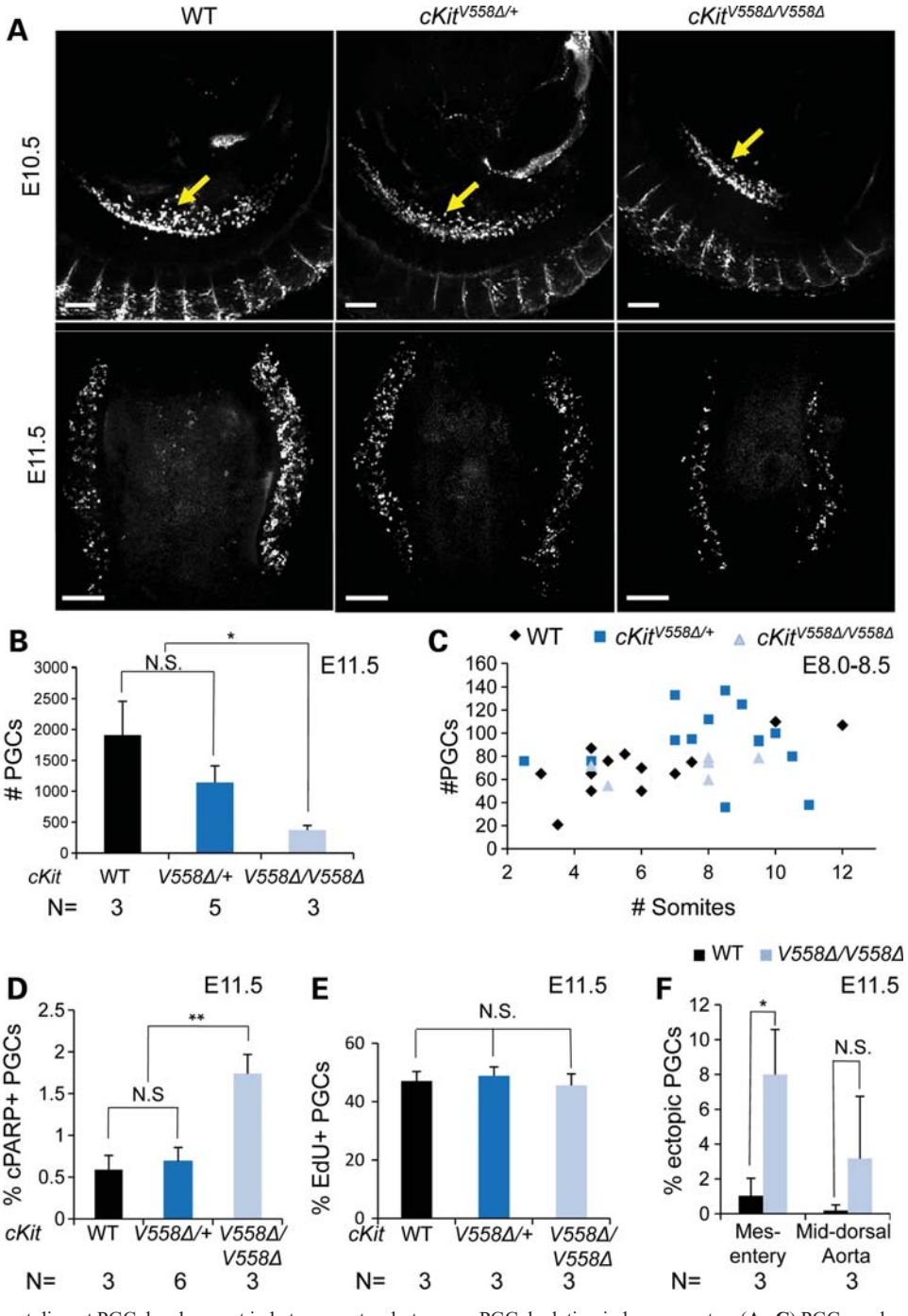

Figure 1. *cKit*$^{V558\Delta}$ does not disrupt PGC development in heterozygotes, but causes PGC depletion in homozygotes. (**A**–**C**) PGC numbers are comparable among WT, *cKit*$^{V558\Delta/+}$ and *cKit*$^{V558\Delta/V558\Delta}$ embryos at E10.5 by SSEA1 staining (arrows, A, top panels), but GCNA staining at E11.5 reveals a severe PGC reduction in the gonads of *cKit*$^{V558\Delta/V558\Delta}$ mutant embryos (A, bottom panels, quantified in B). Analysis of E8.0–8.5 embryos by AP staining confirms that early PGC numbers are similar between WT and *cKit*$^{V558\Delta/V558\Delta}$ embryos, but slightly increased in heterozygotes ($P < 0.05$, C). (**D**) Increased apoptosis in *cKit*$^{V558\Delta/V558\Delta}$ gonads at E11.5 was observed by cPARP staining. (**E**) Similar rates of PGC proliferation in all genotypes were observed by EdU incorporation. (**F**) The frequency of ectopic PGCs in dorsal mesentery was increased in *cKit*$^{V558\Delta/V558\Delta}$ embryos at E11.5. Scale bars = 200 μm. $^{*}P < 0.05$; $^{**}P < 0.01$. Bars represent the mean ± SEM.

Collectively, these phenotypes most resemble null alleles of *cKit* (5,6) and *KitL* (32) and suggest that *cKit*^{S830R} acts as a null allele, possibly with some dominant negative activity. Compared with *cKit*^{S830R}, the *cKit*$^{V558\Delta}$ phenotype in the PGC compartment is significantly milder with later onset.

cKit$^{V558\Delta}$ behaves as loss-of-function allele for PGCs but not for tumor formation

The surprising PGC reduction in *cKit*$^{V558\Delta/V558\Delta}$ mutants raises two distinct possibilities. If PGC survival requires moderate levels of cKit signaling, persistent and excessive activation of

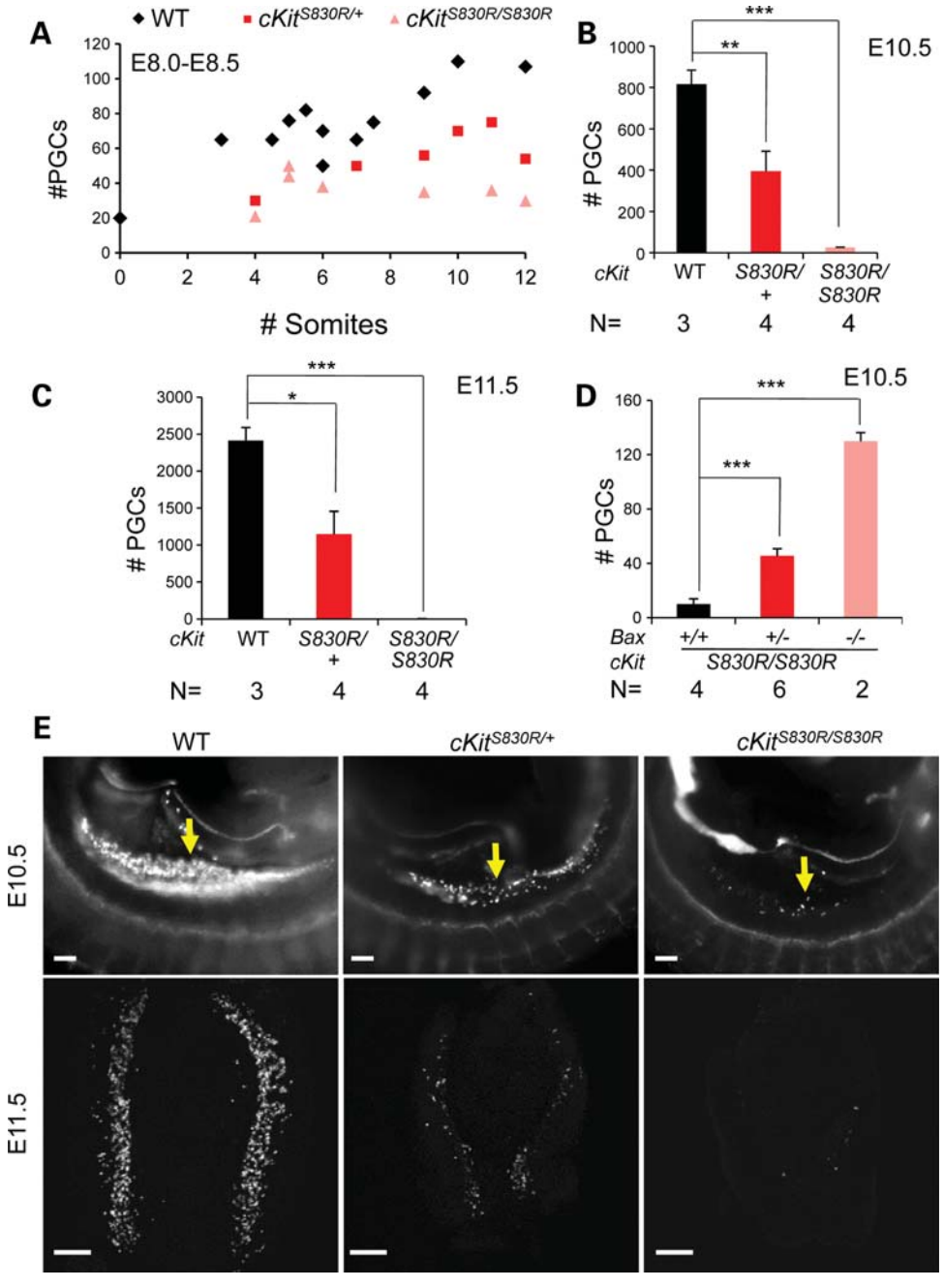

Figure 2. *cKit*^{S830R} is a strong loss of function allele. (**A**) AP staining revealed a decrease in PGC number during early migration at E8.0–8.5 in *cKit*$^{S830R/S830R}$ ($P < 0.001$) embryos. (**B**, **C** and **E**) PGC depletion in both *cKit*$^{S830R/+}$ and *cKit*$^{S830R/S830R}$ was evident by SSEA1 staining (E, arrows), and when quantified was statistically significant at E10.5 (B) and E11.5 (C). (**D**) Removal of one or two Bax alleles significantly rescues PGC loss of *cKit*$^{S830R/S830R}$ embryos. Scale bars = 200 μm. $^{*}P < 0.05$; $^{**}P < 0.01$; $^{***}P < 0.001$. Bars represent the mean ± SEM.

the receptor may be harmful and lead to PGC depletion. Alternatively, *cKit*$^{V558\Delta/V558\Delta}$ may function as a loss-of-function allele for PGCs. To distinguish between these possibilities, we performed three genetic experiments.

First, we crossed *cKit*$^{V558\Delta/+}$ to our ENU loss of function allele, *cKit*$^{S830R/+}$. If PGC depletion in *cKit*$^{V558\Delta/V558\Delta}$ mutants arises from excessive cKit signaling, we might expect a reduction in the level of active cKit to rescue the phenotype in compound heterozygotes. Instead, we observed that PGCs were nearly absent (<10 at E11.5) in *cKit*$^{V558\Delta/S830R}$ embryonic gonads, in contrast to the partial reduction in *cKit*$^{S830R/+}$ and variable though statistically insignificant reduction of PGCs in *cKit*$^{V558\Delta/+}$ embryos at E11.5 (Fig. 3A). Compound heterozygotes were viable, and their germ cell deficiency persisted; by 12 weeks after birth, the gonads were very small, with testes seminiferous tubes sparsely populated or devoid of sperm, and *cKit*$^{V558\Delta/S830R}$ ovaries containing mainly luteinized interstitial cells and few immature and unhealthy

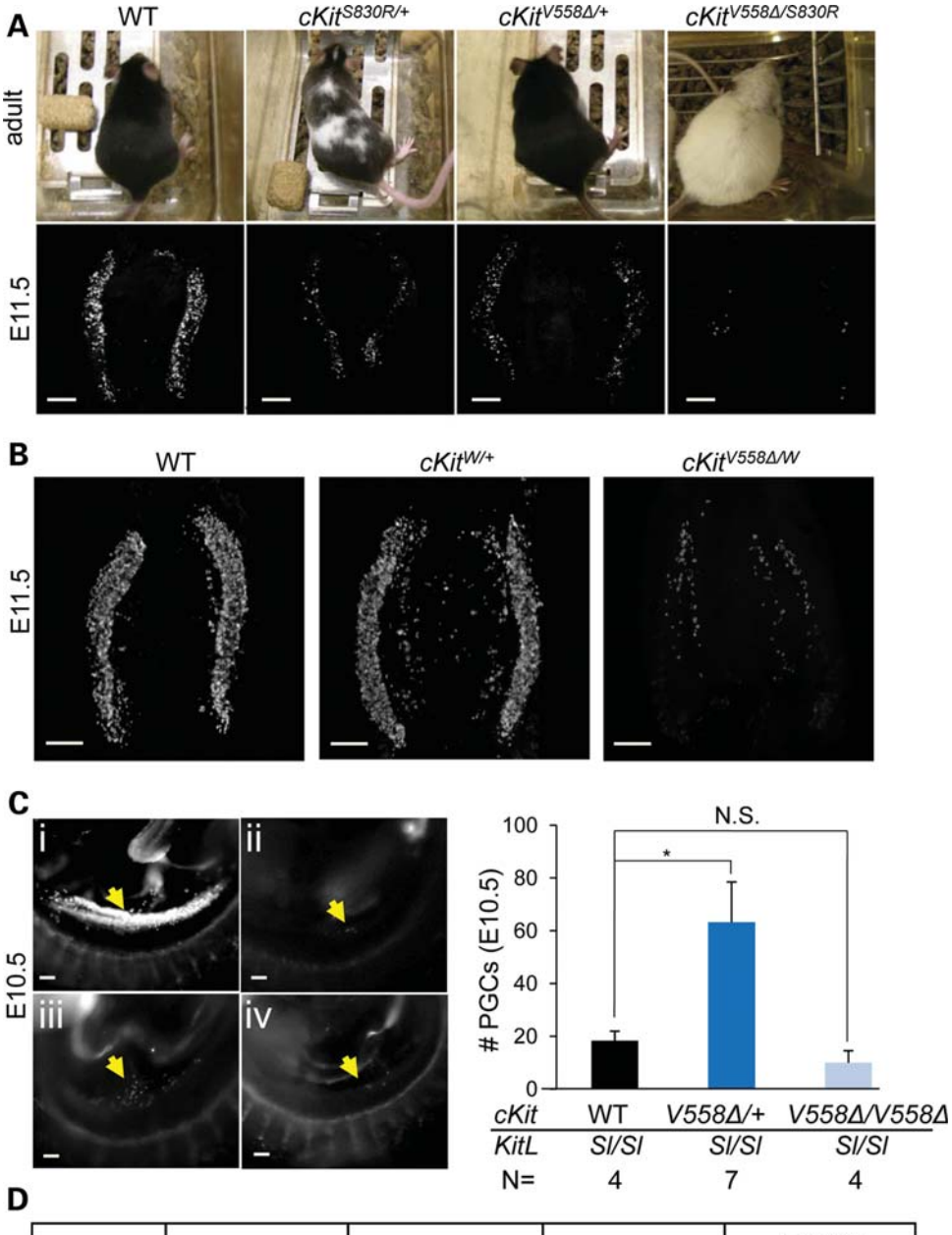

D

	cKit V558Δ/+	cKit V558Δ/S830R	cKit V558Δ/W	cKit V558Δ/+; KitL Sl/+
PGC phenotype	No significant reduction	Nearly absent	Severe reduction	Variable reduction
GIST incidence	100% (20/20)	100% (5/5)	100% (4/4)	100% (10/10)

Figure 3. $cKit^{V558\Delta}$ behaves as a loss-of-function allele for PGCs but not for tumor formation. (**A**) Melanocyte and PGC deficits are more severe in $cKit^{V558\Delta/S830R}$ mice than in $cKit^{S830R/+}$ mice. Coat colors of WT, $cKit^{S830R/+}$, $cKit^{V558\Delta/+}$ and $cKit^{V558\Delta/S830R}$ adult mice on the C57/Bl6 background are shown in top panels. E11.5 gonads were immunostained with SSEA1 (bottom panels). (**B**) In $cKit^{W/V558\Delta}$ E11.5 gonads, stained with SSEA1, PGCs are severely depleted (approximately 200 PGCs/embryo), whereas a variable but statistically insignificant PGC reduction was observed in $cKit^{W/+}$. (**C**) PGCs (arrows), identified by SSEA1 immunostaining, are nearly absent in $KitL^{Sl/Sl}$ embryos (ii, 18 ± 3.6 PGCs). The presence of one $cKit^{V558\Delta}$ allele partially restores PGCs (iii, 67 ± 15). However, $cKit^{V558\Delta/V558\Delta}$ does not rescue PGC depletion in $KitL^{Sl/Sl}$ embryos (iv, 10 ± 7.8 PGCs). WT littermate is shown in (i). (**D**) PGC phenotypes, determined at E11.5, and GIST incidence, examined at 8–12 weeks of age, are summarized in $cKit^{V558\Delta/+}$ mice and compound mutants generated with $cKit^{S830R/+}$, $cKit^{W/+}$ or $KitL^{Sl/+}$. Scale bars = 200 μm. $^{*}P < 0.05$; bars represent the mean ± SEM.

follicles (Supplementary Material, Fig. S4). We also observed a surprising coat color phenotype in this cross, as $cKit^{V558\Delta/S830R}$ adults on C57/Bl6 background were albino, in contrast to the piebaldism of $cKit^{S830R}$ heterozygotes and lack of defect in $cKit^{V558\Delta/+}$ melanocytes (Fig. 3A). The observed germ cell and coat color phenotypes could suggest synergistic inhibitory effects of $cKit^{V558\Delta}$ and $cKit^{S830R}$. However, we cannot rule out the possibilities that $cKit^{S830R}$ exerts dominant negative activity, or that $cKit^{V558\Delta}$ requires dimerization with a wild-type cKIT protein for gain-of-function activity. In order to test these possibilities, we performed a second cross between $cKit^{V558\Delta/+}$ and a null allele, $cKit^{W}$, which abolishes cell-surface expression and kinase activity of the receptor (34). Compound heterozygotes should, therefore, express only $cKit^{V558\Delta}$ homodimers, but at a level 50% of $cKit^{V558\Delta/V558\Delta}$. *W* heterozygotes are identified postnatally by their coat color defects, but the amount of tissue from embryos precluded genotyping by Southern blot. We observed in three litters from $cKit^{V558\Delta/+}$ and $cKit^{W/+}$ parents that 5 out of 21 (24%) embryos exhibited a severe PGC reduction (Fig. 3B); all of these five embryos harbored the $cKit^{V558\Delta}$ allele and occurred at the expected ratio of compound heterozygotes (25%). The PGC deficiency of these presumed compound heterozygotes was milder than that of $cKit^{V558\Delta/S830R}$ and more severe than $cKit^{V558\Delta/V558\Delta}$, corroborating the possibility of $cKit^{S830R}$ dominant negative activity. However, the persistence of approximately 200 PGCs in $cKit^{V558\Delta/W}$ compared with 0–50 in mutants where cKit activity is completely abolished, such as in $cKit^{W/W}$ (5), suggests a low level of signaling from $cKit^{V558\Delta}$ homodimers in PGCs.

To determine whether $cKit^{V558\Delta}$ activity in PGCs depends upon KitL or is ligand-independent, we generated compound mutants between $cKit^{V558\Delta}$ and a *KitL* null allele, *Steel* (35). An early and profound loss of PGCs occurs in $KitL^{Sl/Sl}$ embryos (32), and thus we predicted that any cKit receptor autoactivity in PGCs should mollify this loss. Compared with background and stage-matched $KitL^{Sl/Sl}$ homozygotes, which have 0–30 PGCs at E10.5, no difference was observed in $cKit^{V558\Delta/V558\Delta};KitL^{Sl/Sl}$ double homozygotes (Fig. 3C), suggesting that $cKit^{V558\Delta/V558\Delta}$ does not have ligand-independent activity in PGCs. Interestingly, on a $KitL^{Sl/Sl}$ null background, $cKit^{V558\Delta/+}$ significantly increases the mean PGC number from 18 to 63 (Fig. 3C), demonstrating a functional consequence for ligand-independent activity in promoting PGC survival. Together, these compound mutants suggest that $cKit^{V558\Delta}$ is responsive to and dependent upon *KitL*, as its genetic ablation significantly impacts PGC phenotypes; furthermore, $cKit^{V558\Delta}$ exhibits no basal or ligand-independent activity in PGCs when homozygous, and when heterozygous, is capable of low levels of autoactivity.

In three different genetic contexts, homozygous *V558Δ* behaves as a loss-of-function rather than a gain-of-function allele in PGCs. However, one allele of *V558Δ* appears to be sufficient for the development of GISTs on any genetic background; masses were observed in the cecum of 100% of $cKit^{V558\Delta/S830R}$, $cKit^{V558\Delta/W}$ and $cKit^{V558\Delta/+};KitL^{Sl/+}$ adults at ages of 8–12 weeks (Fig. 3D). Whereas GIST development appears to be unaffected by reduced dosage of *KitL*, reduced levels of *cKit* or homodimerization of *V558Δ*, PGC development is highly compromised. Collectively, these phenotypes reveal distinct and cell-context-specific cKit signaling requirements between GISTs and PGCs.

Pluripotent EGCs derived from $cKit^{V558\Delta}$ mutant PGCs recapitulate the phenotype

In light of the limitations to conducting biochemistry with PGCs, we chose to study signaling mechanisms in $cKit^{V558\Delta}$ mutants in an immortal cell line that most closely approximates PGCs in lineage and expression. We derived lines of EGCs from E11.5 PGCs bearing the Oct4ΔPE:EGFP reporter and established lines of wild-type, $cKit^{V558\Delta/+}$ and $cKit^{V558\Delta/V558\Delta}$ EGCs (Fig. 4A) (3,4,36). Maintained in self-renewing conditions, EGCs from all genotypes exhibited similar rates of proliferation, measured by BrdU incorporation (Supplementary Material, Fig. S5). By annexin V staining, we observed an increase in apoptosis among $cKit^{V558\Delta/V558\Delta}$ EGCs ($5.43 \pm 1.73\%$) compared with heterozygous ($2.36 \pm 0.37\%$) or wild-type EGCs ($2.14 \pm 0.01\%$; Fig. 4B). This decrease in the survival of $cKit^{V558\Delta/V558\Delta}$ EGCs compared with heterozygote or wild-type EGCs paralleled the trend observed in PGCs (Fig. 1D). We confirmed that all three EGC lines express similar levels of *cKit* transcript (Fig. 4C) as well as total cKIT protein (Fig. 4D), eliminating the possibility of variability due to cKit expression levels.

We next assessed cell-surface expression of cKIT in mutants, since activity-induced endocytosis is a well-known negative feedback mechanism for cKit (37). Flow cytometric comparison of cKIT expression at the cell surface revealed a moderate reduction in $cKit^{V558\Delta/+}$ EGCs and even greater reduction in $cKit^{V558\Delta/V558\Delta}$ EGCs (Fig. 4E). We wondered whether progressively reduced surface cKIT in *V558Δ* heterozygous and homozygous EGCs reflects increased receptor autoactivity, and furthermore whether this attenuation mechanism affects subsequent ligand sensitivity. To assay the ligand responsiveness of each EGC genotype, we pulsed with 60 ng/ml soluble KitL (SCF); a corresponding decrease in cKIT surface expression was observed after 30 min of SCF treatment, and this relative decrease was identical in wild-type, $cKit^{V558\Delta/+}$ and $cKit^{V558\Delta/V558\Delta}$ EGCs despite the initially different levels (Fig. 4F). We sought to validate these discrepancies in EGC cKIT expression *in vivo*, and similarly found in E11.5 PGCs that the down-regulation in $cKit^{V558\Delta/+}$ and further in $cKit^{V558\Delta/V558\Delta}$ was comparable with that in EGCs (Fig. 4G). In contrast, we observed that $cKit^{S830R/+}$ PGCs exhibit wild-type levels of cKIT protein on cell surface (Fig. 4H), suggesting differences in mutant receptor signaling or trafficking between $cKit^{V558\Delta}$ and $cKit^{S830R}$. These results establish the use of EGCs as a relevant tool for studying *V558Δ* mutant receptor activity; together with the $cKit^{V558\Delta};KitL^{Sl/Sl}$ cross, these studies indicate normal ligand-responsiveness but compromised signaling or trafficking of $cKIT^{V558\Delta}$ in EGCs and PGCs.

AKT is highly activated in GISTs but remains unperturbed by $cKit^{V558\Delta}$ in EGCs and PGCs

Crosses with two *cKit* LOF alleles as well as *KitL* revealed different behavior of *V558Δ* in tumors versus PGCs and ruled out the possibility that excessive cKit signaling leads to the

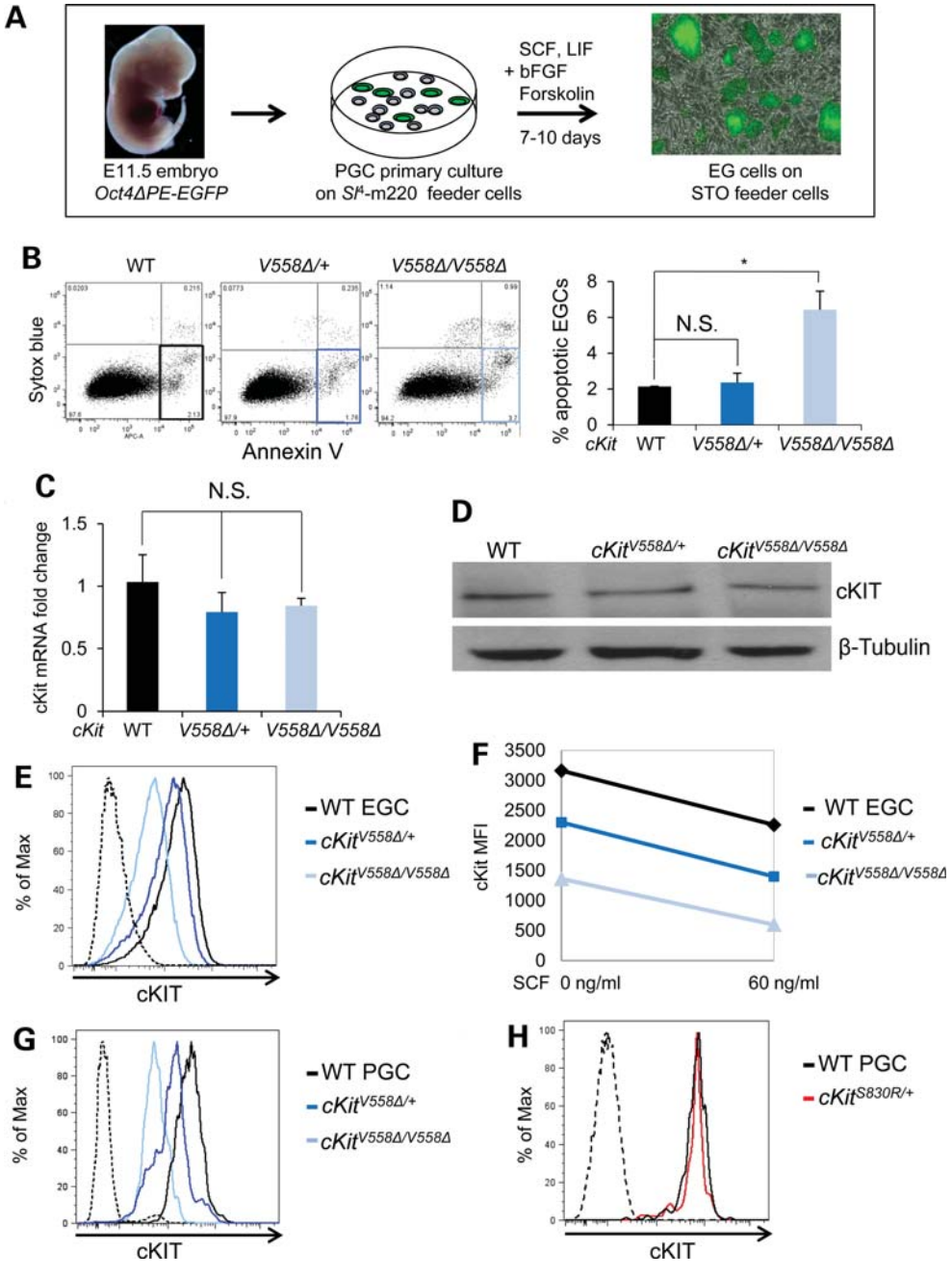

Figure 4. EGCs derived from $cKit^{V558\Delta}$ PGCs recapitulate survival defects and display lower levels of surface cKIT. (**A**) EGC cell lines were derived from PGCs of E11.5 embryos harboring *Oct4ΔPE:GFP* as schematized and cultured on STO feeder cells (gray). (**B**) By annexin V staining, apoptosis was slightly increased in $cKit^{V558\Delta/V558\Delta}$ EGCs compared with WT or heterozygotes. (**C**) Similar levels of *cKit* transcript in all EGC genotypes were verified by qRT-PCR. (**D**) cKIT protein levels did not differ among all EGC genotypes by immunoblotting. (**E**–**H**) Live immunostaining with cKIT antibody revealed successively reduced surface expression on $cKit^{V558\Delta/+}$ and $cKit^{V558\Delta/V558\Delta}$ EGCs. SCF-induced downregulation of cKIT was comparable in all EGC genotypes (F). Similarly, cell surface cKIT reduction was observed in $cKit^{V558\Delta/+}$ and $cKit^{V558\Delta/V558\Delta}$ PGCs (G) but not on $cKit^{S830R/+}$ PGCs (H). $^{*}P < 0.05$; bars represent mean ± SEM.

demise of PGCs. These genetic studies suggest that PGC loss in *V558Δ* homozygotes occurs by a different, loss-of-function mechanism. We next used the EGCs to interrogate phosphorylation of candidate downstream signaling molecules biochemically. Hyperphosphorylation of AKT was previously reported in GISTs from $cKit^{V558\Delta/+}$ mice, and markedly decreased following imatinib-induced tumor regression (38). We first compared AKT phosphorylation between EGCs derived from WT PGCs and GISTs isolated from $cKit^{V558\Delta/+}$ mice by western blot (Fig. 5A). Consistent with previous studies (38), we observed a high level of AKT protein expression and phosphorylation in GIST tumor lysates relative to wild-type EGCs. Upon comparing AKT phosphorylation in WT and $cKit^{V558\Delta}$ EGCs, we observed uniform levels among all genotypes in the absence of added SCF, and similar P-AKT increases following SCF stimulation (Fig. 5B). In E11.5 sections, we

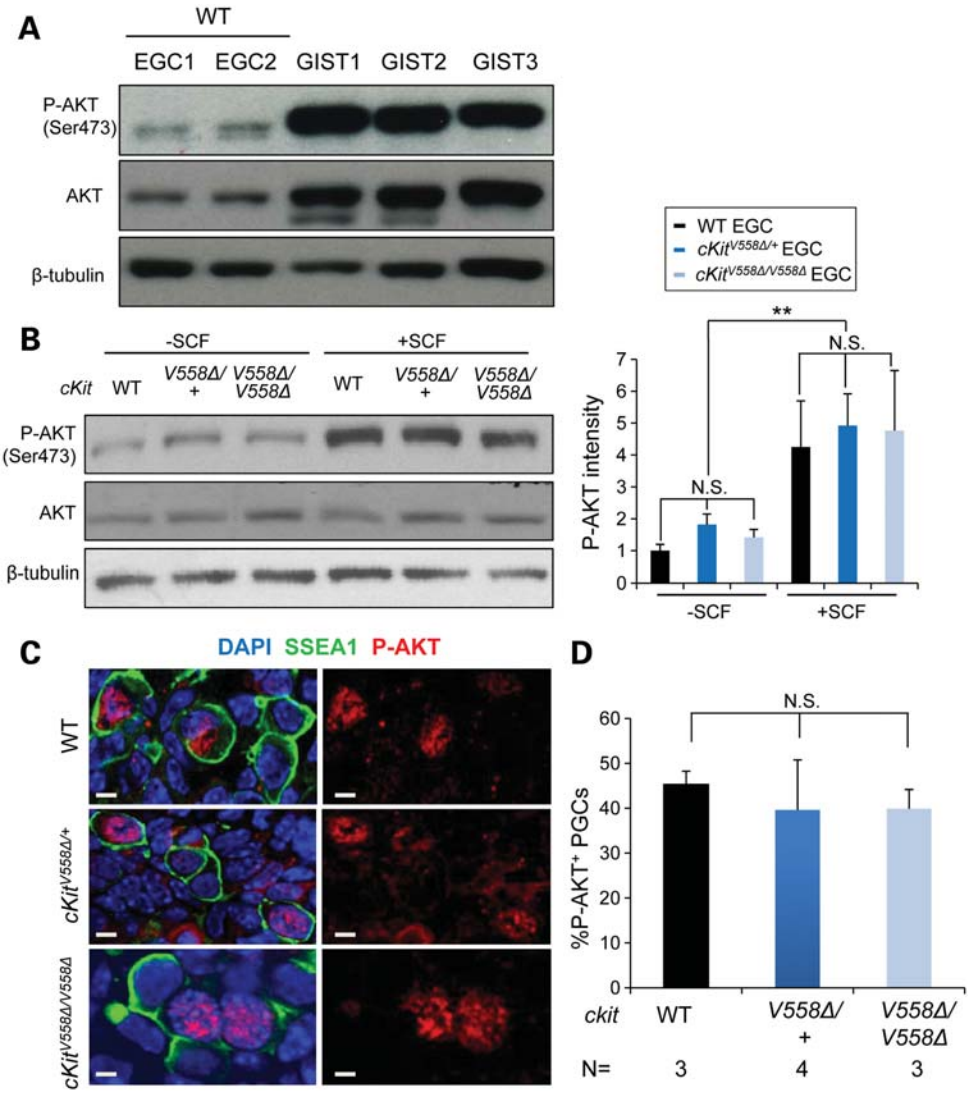

Figure 5. P-AKT signaling is intact in $cKit^{V558\Delta/V558\Delta}$ PGCs and EGCs. (**A**) Cell lysates of GISTs from three $cKit^{V558\Delta/+}$ mice immunoblotted with anti-phospho-AKT (Ser 473) antibody followed by anti-pan AKT antibody, and anti-β-tubulin antibody showed elevated P-AKT and robust total AKT compared with EGCs. (**B**) EGCs sorted from STO feeder cells were starved for 2 h and then treated with 50 ng/ml SCF for 10 min. Immunoblotting revealed similar AKT phosphorylation across genotypes. The P-AKT levels that are shown on the graphs have been normalized to total AKT in $n = 3$ experiments. (**C** and **D**) P-AKT immunostaining in E11.5 embryo sections revealed nuclear signal in a subset of PGCs, identified by SSEA1 immunostaining (C). The frequency of P-AKT$^+$ PGCs was similar among all genotypes (D). Scale bars = 5 μm. $^{**}P < 0.01$. Bars represent the mean ± SEM.

detected robust P-AKT immunoreactivity in the nuclei of approximately half of PGCs (Fig. 5C); cytoplasmic P-AKT was not observed in PGCs, but was present in other somatic cells. However, the frequency of P-AKT-positive PGCs did not differ between wild-type, heterozygotes and homozygotes (Fig. 5D). This result suggests, first, that altered AKT signaling does not underlie the loss of PGCs in $cKit^{V558\Delta/V558\Delta}$, and, second, that $cKit^{V558\Delta/+}$ does not elevate AKT activity in PGCs as in GISTs, and presumably their precursors (38).

We also examined several effectors of the JAK-STAT pathway, of which only P-STAT-3 could be detected in EGCs. As shown in Supplementary Material, Figure S6, we observed a moderate increase of STAT-3 phosphorylation in $cKit^{V558\Delta/+}$, but no alteration in $cKit^{V558\Delta/V558\Delta}$ EGCs.

Loss of MAPK signaling compromises the survival of $cKit^{V558\Delta/V558\Delta}$ mutant PGCs

We next examined effectors of the MAPK pathway in EGCs and PGCs. By immunoblotting, we confirmed that ERK was consistently more activated in GISTs from $cKit^{V558\Delta/+}$ mice compared with EGCs (Fig. 6A). ERK phosphorylation was similar between wild-type and $cKit^{V558\Delta/+}$ EGCs in the absence of exogenous SCF, whereas phosphorylation was markedly reduced in $cKit^{V558\Delta/V558\Delta}$ EGCs (Fig. 6B). This persistence of ERK1/2 activity may be attributable to autocrine SCF production by EGCs, which we noted by qRT-PCR (data not shown). Following SCF addition, ERK1/2 phosphorylation increased modestly in $cKit^{V558\Delta/V558\Delta}$ EGCs, but

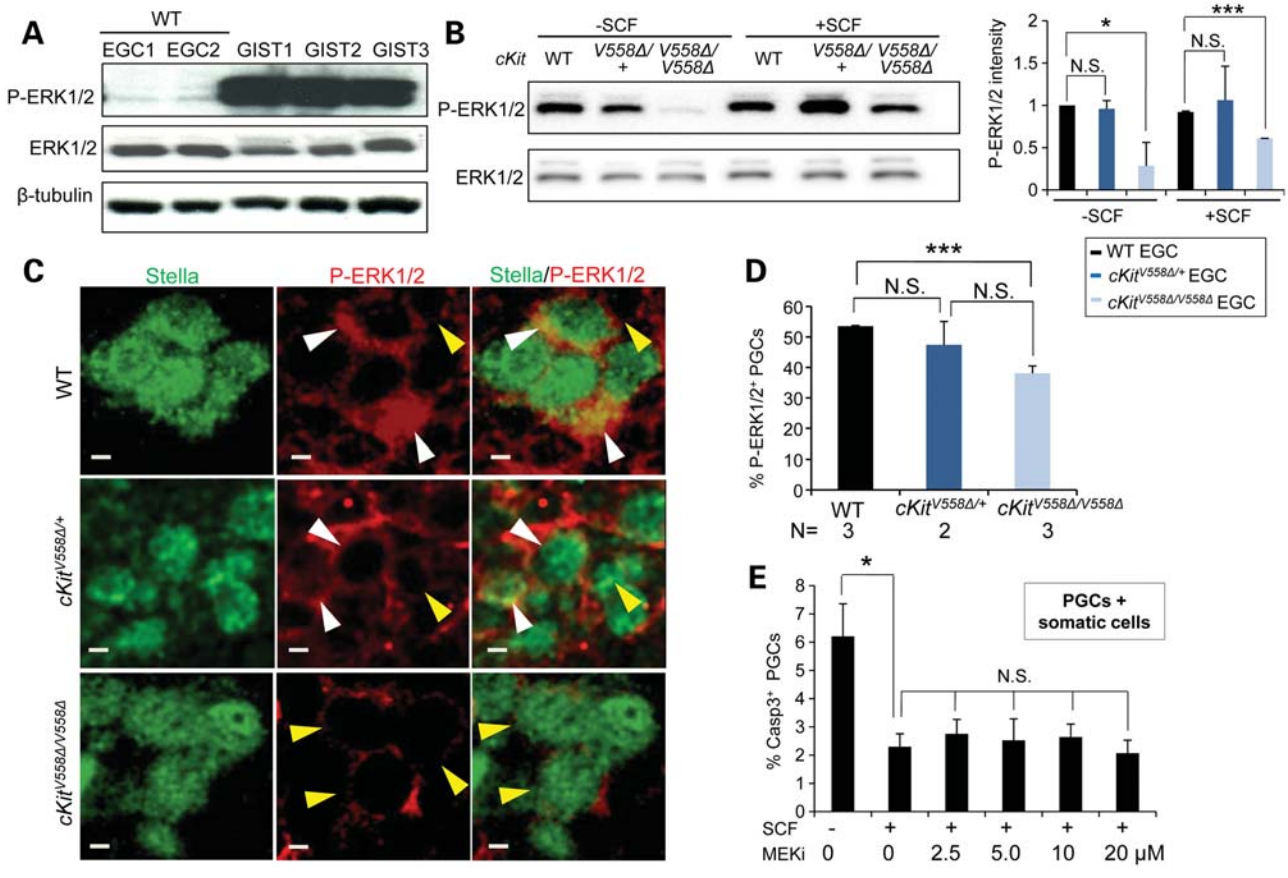

Figure 6. Hypophosphorylation of ERK1/2 in $cKit^{V558\Delta/V558\Delta}$ PGCs and EGCs. (**A**) GISTs (from three $cKit^{V558\Delta/+}$ mice) and cell lysates isolated from sorted EGCs (WT, two lines) were immunoblotted for P-ERK1/2, total ERK1/2 and β-tubulin, revealing high levels of activated ERK in GISTs. (**B**) EGCs sorted from STO cells were starved for 2 h and then treated with 50 ng/ml SCF for 10 min. Immunoblotting revealed a decrease in ERK1/2 phosphorylation in $cKit^{V558\Delta/V558\Delta}$. The P-ERK1/2 levels shown on the graphs have been normalized to total ERK1/2. (**C**) WT, $cKit^{V558\Delta/+}$ and $cKit^{V558\Delta/V558\Delta}$ embryos at E11.5 were sectioned and co-immunostained for P-ERK1/2 and Stella, a PGC marker. P-ERK1/2 (red), mainly detected in cytoplasm and occasionally in the nucleus, was strong (white arrow heads) in WT and heterozygous PGCs, whereas it was weak or absent (yellow arrow heads) in $cKit^{V558\Delta/V558\Delta}$ PGCs. Frequencies of P-ERK1/2-positive PGCs (exhibiting strong staining) were quantified (**D**). (**E**) PGC from E11.5 WT embryos were co-cultured with somatic gonad cells in DMEM with 50 ng/ml SCF and an MEK inhibitor, PD032590, at the indicated concentrations for 20 h. The frequency of apoptotic PGCs, detected by caspase-3 and SSEA1 co-immunostaining, did not increase with MEK inhibitor treatment. Scale bars = 5 μm. $^{*}P < 0.05$, $^{***}P < 0.001$.

remained significantly lower than that of wild-type or heterozygote. We sought to validate these ERK phosphorylation differences in PGCs by immunohistochemistry. In E11.5 sections, P-ERK1/2 was primarily detected in cytoplasm and occasionally in the nucleus of PGCs within the gonad, in 56.4% of wild-type PGCs (Fig. 6C and D), consistent with a previous report (39). $cKit^{V558\Delta/+}$ PGCs did not differ from wild-type in ERK phosphorylation. However, in $cKit^{V558\Delta/V558\Delta}$, P-ERK1/2 immunoreactivity was much weaker and could be scored in only 36.7% of PGCs (Fig. 6C and D); this result *in vivo* corroborates the P-ERK1/2 loss observed in $cKit^{V558\Delta/V558\Delta}$ EGCs. We tested the effect of P- ERK1/2 loss by culturing wild-type E11.5 PGCs in an MEK inhibitor, PD0325901. However, at a range of doses, programmed cell death was not increased in either PGCs co-cultured with somatic cells (Fig. 6E) or purified PGCs (data not shown); these studies could suggest that cKIT-mediated ERK1/2 signaling is not critical for PGC survival.

We next examined the activity of JNK, another important MAPK that mediates mast cell proliferation via SCF (40). In EGCs, phosphorylation of JNK1 was diminished in $cKit^{V558\Delta/V558\Delta}$ compared with that in wild-type or heterozygote (Fig. 7A). Examination of GISTs from $cKit^{V558\Delta/+}$ mice revealed, in contrast, undetectable levels of JNK phosphorylation compared with EGCs (Fig. 7B). By immunofluorescence, we were able to detect phosphorylated JNK in E11.5 cultured PGCs. Whereas a punctate nuclear signal was observed in wild-type and heterozygotes, the intensity of P-JNK was significantly reduced in $cKit^{V558\Delta/V558\Delta}$ PGCs; quantitation of this signal in confocal stacks corroborated a highly significant reduction of P-JNK in homozygous PGCs and a possible decrease in heterozygotes (Fig. 7C). Since JNK has not been previously implicated in PGC development, we began with an assay of its function in E11.5 PGCs co-cultured with somatic cells and exogenous SCF. Addition of a JNK inhibitor (JNKi), SP600125, significantly increased apoptosis in a dose-dependent fashion (Fig. 7D). Primary PGCs purified from E11.5 WT embryos responded similarly to the JNKi (data not shown), suggesting that JNK acts autonomously in PGCs to promote their survival. $cKit^{V558\Delta/V558\Delta}$

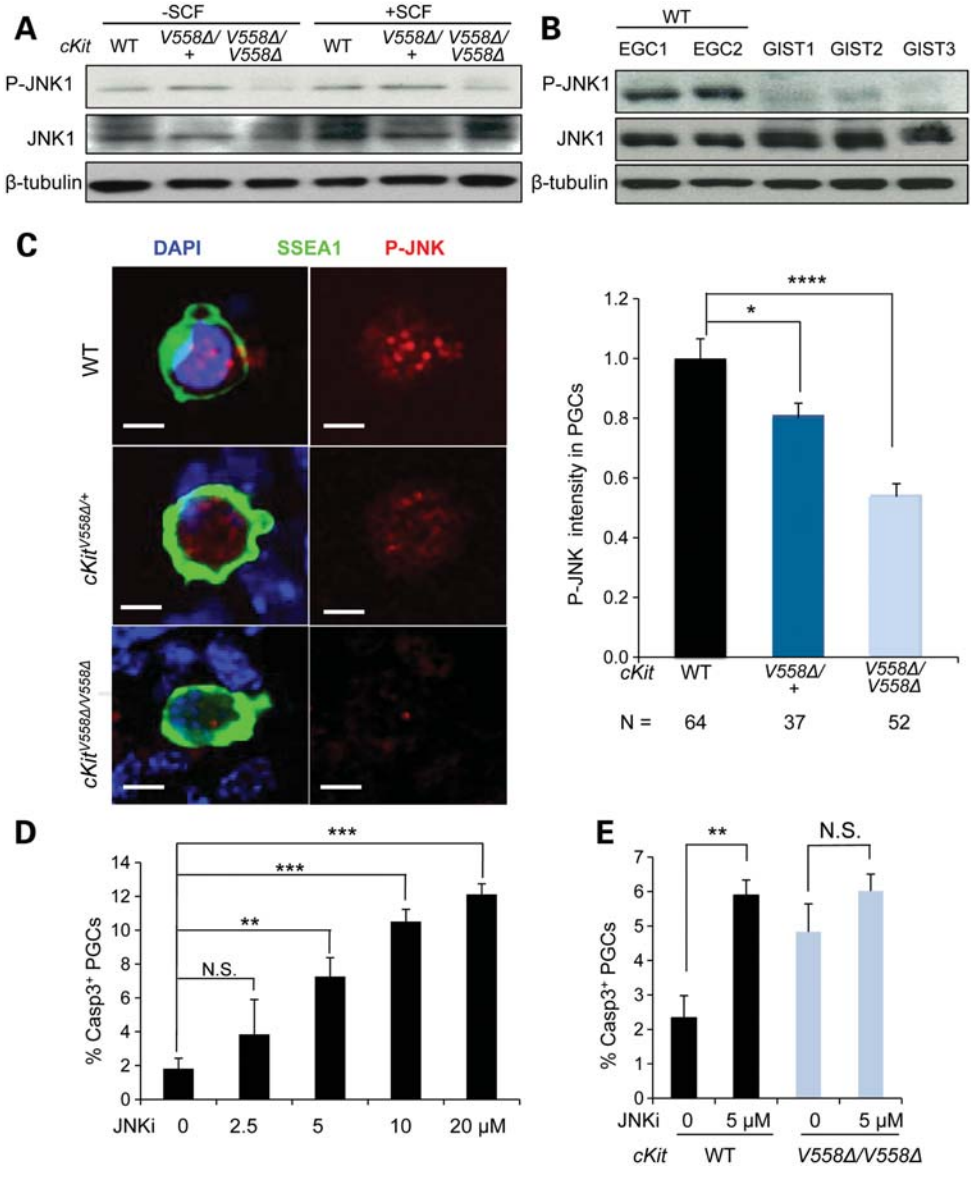

Figure 7. Loss of JNK signaling compromises the survival of $cKit^{V558\Delta/V558\Delta}$ mutant PGCs. (**A**) EGCs sorted from STO cells were starved for 2 h and then treated with 50 ng/ml SCF for 10 min. Immunoblotting for P-JNK, total JNK and β-tubulin showed a decrease in JNK1 phosphorylation in $cKit^{V558\Delta/V558\Delta}$ EGCs. (**B**) Lysates of GISTs from three $cKit^{V558\Delta/+}$ mice were compared with cell lysates isolated from sorted EGCs (WT, two lines) by immunoblotting. P-JNK was not reliably detected in GIST lysates. (**C**) Gonadal cells from E11.5 WT, $cKit^{V558\Delta/+}$ or $cKit^{V558\Delta/V558\Delta}$ embryos were cultured for 20 h before P-JNK and SSEA1 co-immunostaining. P-JNK immunolocalized to the nuclei of PGCs and appeared reduced in $cKit^{V558\Delta/V558\Delta}$ PGCs, as shown by quantification of P-JNK intensity. Scale bars = 5 μm. (**D**) Gonadal cells from E11.5 WT embryos were cultured in DMEM with 50 ng/ml SCF at the indicated concentrations of a JNKi, SP600125, for 20 h. Apoptotic PGCs were detected by co-immunostaining with SSEA1 and caspase 3, with DMSO as a vehicle control. The JNKi increased PGC apoptosis in a dose-dependent manner. (**E**) PGCs cultured with gonadal somatic cells of E11.5 WT or $cKit^{V558\Delta/V558\Delta}$ embryos were treated with 5 μM JNKi for 20 h in the presence of 50 ng/ml SCF. The JNKi increased apoptosis of WT PGCs, but not $cKit^{V558\Delta/V558\Delta}$ PGCs. $^{**}P < 0.01$, $^{***}P < 0.001$, $^{****}P < 0.0001$. Bars represent mean ± SEM.

PGCs cultured without JNKi exhibited similarly elevated levels of apoptosis. Importantly, the addition of JNKi did not further increase apoptosis of $cKit^{V558\Delta/V558\Delta}$ PGCs in culture (Fig. 7E).

Together, our data raise the possibility that cKit-mediated JNK signaling promotes PGC survival but acts independently of ERK1/2. These results demonstrate the suppression of two MAPK effectors in $cKit^{V558\Delta/V558\Delta}$ EGCs as well as PGCs and show that pharmacologic inhibition of JNK induces PGC apoptosis. The pronounced difference between the phosphorylation state of both ERK and JNK in EGCs and GISTs underscores the distinct and cell-context-specific cKit signaling requirements suggested by our genetic experiments.

DISCUSSION

KitL-cKit is the most critical growth factor signaling pathway for mammalian PGCs, as its disruption produces the most

severe effects on PGC survival. In this report, we used an oncogenic cKit gain-of-function mutation, *V558Δ*, to study the consequences of overactivated cKit for PGC development. Contrary to phenotypes in mast cells and intestine, we find that $cKit^{V558\Delta}$ does not cause PGC overgrowth; whereas GISTs arising in heterozygotes have been associated with hyperactive AKT and ERK signaling (18,38,41), normal levels found in EGCs and PGCs argue for the existence of mechanisms that buffer cKit signaling. Surprisingly, *V558Δ* homozygosity leads to apoptotic attrition of PGCs and EGCs and the attenuation of MAPK signaling. Our work suggests that loss of JNK underlies PGC death in $cKit^{V558\Delta/V558\Delta}$ and that JNK is a previously unrecognized mediator of PGC survival via cKit. Together, these results underscore the distinct and cell-context-specific management of the KitL-cKit signaling pathway.

First and foremost, this work reveals unusual behavior of an oncogenic, autoactivating allele in PGCs. $cKit^{V558\Delta}$ has been established as a gain-of-function mutation in mast cells and interstitial cells of Cajal, where it produces hyperproliferation or hyperplasia (18,38,42). Contrary to expectation, our analysis in PGCs revealed loss-of-function behavior of this mutant: when homozygous and in trans with two *cKit* loss-of-function alleles, $cKit^{S830R}$ and $cKit^{W}$, $cKit^{V558\Delta}$ caused a reduction in PGCs by E11.5, whereas GISTs still formed. Similar cell-context-dependent properties of cKit signaling have been described for a number of other alleles (28,43). Examination of $cKit^{V558\Delta}$ phenotypes in the *KitL* null genetic background, in which ligand is absent, supports the notion that $cKit^{V558\Delta}$ lacks autoactivity in PGCs when homozygous, as the double mutants phenocopy the virtual absence of PGCs in *KitL* single mutants. However, the partial rescue of $KitL^{Sl/Sl}$ PGCs by one *V558Δ* allele indicates a different phenomenon in the heterozygote. This result could suggest that $cKit^{V558\Delta}$ autoactivity in PGCs requires the presence of a wild-type *cKit* allele. On balance, the $cKit^{V558\Delta/+}$-mediated PGC increase is significant in a $KitL^{Sl/Sl}$ background, but corresponds in numbers to ∼6% of the total PGC population in wild-type at E10.5; a 6% increase in PGCs would not be detected in heterozygotes, which are indistinguishable from wild-type. Alternatively, this demonstrated ligand-independent activity in $KitL^{Sl/Sl};cKit^{V558\Delta/+}$ mutant PGCs could suggest the presence of a molecular overload protector in PGCs that restricts the level of cKit signaling above a threshold. In this case, the persistence of normal PGC development in $cKit^{V558\Delta/+}$ could result from such buffering mechanisms, which are not in effect at low levels of cKit signaling, such as on the *Sl/Sl* background.

Examination of the downstream signaling mediators in EGCs and PGCs corroborates the phenotypes observed in *V558Δ* heterozygotes and homozygotes. Previous biochemical studies of *V558Δ* focused on GISTs, cultured bone-marrow-derived mast cells or overexpression in cell lines, but signaling has not been examined in normal tissues (18,38,41). $cKit^{V558\Delta/+}$ EGCs exhibited levels of AKT and ERK1/2 phosphorylation comparable with wild-type. Although STAT3 phosphorylation was elevated, this apparently does not affect rates of proliferation and apoptosis in $cKit^{V558\Delta/+}$ EGCs, which were identical to wild-type. Many studies of GISTs, including the $cKit^{V558\Delta/+}$ mouse model, point to active AKT and ERK pathways as critical for tumor growth (18,38,41,44,45). Therefore, the unaltered levels of both mediators in $cKit^{V558\Delta/+}$ EGCs is striking, particularly in comparison with the high AKT and ERK phosphorylation in GISTs. In PGCs, AKT phosphorylation occurs rapidly upon the addition of SCF (11) and has been associated with survival and cell-cycle regulation (46–49). However, our direct *in vivo* examination of phospho-AKT in PGCs confirmed that the levels of response remain unaffected by *V558Δ*. The discrepancy between AKT activation in $cKit^{V558\Delta/+}$ GISTs and EGCs/PGCs reinforces the idea of a germ-cell-specific mechanism for attenuating high levels of PI3K signaling. Perhaps consistent with this notion, *in vivo* PGC development was not disrupted in a mouse engineered for increased AKT activation that had activity even in the absence of tamoxifen (47). The basis of this proposed buffering mechanism in PGCs, or its loss in tumor cells, will be important future questions.

The state of signaling in $cKit^{V558\Delta/V558\Delta}$ EGCs and PGCs sharply diverged from that in heterozygotes. As might be predicted by the loss-of-function phenotypes, *V558Δ* homozygotes exhibited reduced phosphorylation of the MAP kinases ERK1/2 and JNK1 compared with either wild-type or heterozygotes. Although it may be tempting to speculate that reduced cKIT cell-surface expression in homozygotes contributes to this signaling deficiency, this relationship is unclear, as cKit alleles with aberrant trafficking can contribute to signaling from within subcellular compartments (50,51). MAP kinase signaling remains largely unstudied in PGCs. Work in a fibroblast growth factor receptor 1 mutant demonstrated a reduction in both PGC survival and ERK1/2 activation, but did not establish a causal connection (39). Despite the observed loss of ERK1/2 phosphorylation in EGCs and PGCs *in vivo*, 20 h culture of PGCs with an MEK inhibitor did not recapitulate the PGC apoptosis phenotype of $cKit^{V558\Delta/V558\Delta}$. Although in a previous report MEK inhibitor diminished PGC numbers after 7 days in culture, by this point the remaining cells likely underwent transformation to EGC colonies, which may respond differently (48). Our studies diminish the possibility that ERK signaling promotes PGC survival in the E11.5 gonads within the observed time frame. However, ERK likely mediates other functions of PGCs downstream of cKit, such as migration, as suggested by *in vitro* studies with the MEK inhibitor (11). Alternatively, recent demonstration that ERK inhibition preserves the naïve pluripotent state and enhances EGC derivation suggests, tantalizingly, that cKit-mediated ERK signaling promotes differentiation of PGCs in the gonad (52).

Our studies of $cKit^{V558\Delta/V558\Delta}$ more clearly implicate another MAP kinase, JNK, in promoting PGC survival via cKit. Numerous studies paradoxically link the JNK pathway to both activation and avoidance of apoptosis, depending on cell type, stimulus, duration of activation and activity of other signaling pathways (53). JNKs are highly activated by cellular stresses such as heat shock, UV and irradiation and by inflammatory cytokines including TNF-α and IL-1. On the other hand, a number of growth factors including EGF, nerve growth factor and SCF induce JNK activation (40,54). For example, in mast cells, irradiation causes slow and sustained JNK activation and concomitant apoptosis, whereas

SCF induces rapid and transient activation of JNKs that promote mast cell proliferation (40). We found that activation of JNK1 was reduced in $cKit^{V558\Delta/V558\Delta}$ EGCs, and in PGCs, a phospho-JNK1/2 antibody revealed a corresponding reduction in homozygotes. Most convincingly, we demonstrated that the JNKi confers death upon wild-type PGCs, but does not further increase apoptosis of $cKit^{V558\Delta/V558\Delta}$ PGCs. A sterility phenotype in mice deficient for JNK ($Jnk1^{-/-}$; $Jnk2^{+/-}$) may support the role of this pathway in germ cell development (55). A pro-survival function of JNK has been reported, and operates through the direct phosphorylation of the proapoptotic mediator BAD, which prevents its association with BclX (56). The expression of BAD in migratory PGCs has been established (7). However, the intriguing localization of phospho-JNK to the nucleus of PGCs could suggest an alternative, transcriptional role. Recent work in differentiating ESCs uncovered a novel function for JNKs as co-regulators of transcription that directly modify histones within promoter regions (57). In contrast to PGCs and EGCs, the absence of JNK activation we observed in GISTs is consistent with previous characterization of GISTs from other genetic models (58) and further underscores the cell-context-specific behavior of $cKit^{V558\Delta}$. The mechanisms and other functions of this newly recognized cKit-JNK axis in PGCs as well as EGC derivation warrant further investigation.

In summary, these studies demonstrate discrete and lineage-specific functions of separate signaling pathways activated by cKit. Our results are consistent with a model in which PGCs depend upon cKit-JNK signaling for their survival and rely upon ERK for other functions. The molecular mechanisms by which these MAP kinases regulate such important functions of early germ cells remain to be elucidated. Evidence for the resistance of PGCs to high levels of cKit signaling raises the question of whether such a mechanism is protective against germ cell tumors.

MATERIALS AND METHODS

Mouse breeding, mapping and genotyping

All animal work was conducted in accordance with protocols approved by the Institutional Animal Care and Use Committee at the University of California, San Francisco. Embryos were generated in timed matings by monitoring for copulatory plugs. $cKit^{V558\Delta}$ mice (MGI:2663995), a gift from Dr P. Besmer, Sloan-Kettering Institute, were genotyped as described (18) and maintained on a mixed C57BL/6-CD1 background to extend the survival of heterozygotes beyond 3 months. Other mouse strains used included $cKit^{W}$ (MGI:1856232), $Kitl^{Sl}$ (MGI:1856161), *Bax* (MGI:1857429) and *Oct4-ΔPE-EGFP* (59), with genotyping performed as described elsewhere (7,60,61). $cKit^{S830R}$ mice were identified in a recessive ENU screen at E9.5 for mouse mutants with PGC defects (12,33). Linkage was established with chromosome 5, using D5MIT15 and D5MIT134 SSLPs, and the *cKit* transcript was PCR-amplified and sequenced from mutant embryo cDNA. $cKit^{S830R}$ mice were subsequently maintained on a C57BL/6 background and genotyped by HinP1 RFLP analysis using the following primers: 5′-GAACCCCTGGACTTCTCTGCTCTT-3′ and 5′-GTGGCAAATCAGTGTCCATGTGGG-3′ (Supplementary Material, Fig. S3).

PGC *ex vivo* culture

The gonad-mesonephri of E11.5 embryos were dissociated with 0.25% trypsin for 3 min followed by 5 mg/ml DNase I. This cell suspension was directly seeded on chambered slides (Lab-Tek II) coated with 1 mg/ml Matrigel or else subjected to flow cytometry for PGC purification and then cultured at 37°C in 5% CO_2 with DMEM/15% knockout serum replacement (KSR) (Invitrogen), 1000 U/ml LIF (Millipore) and 50 ng/ml SCF (Invitrogen) for 20 h. Cells were then fixed in 4% PFA at room temperature and immunostained for P-JNK. For MEK and JNKi experiments, PGCs collected as above or PGCs sorted from gonad-mesonephri were cultured in DMEM medium with 50 ng/ml SCF and an MEK inhibitor, PD-0325901 (Selleck and Stemgent), or a JNKi (SP600125, Calbiochem) for 20 h. Cells were fixed for immunostaining.

EGC derivation and maintenance

EGC lines were derived from E11.5 embryos as described (4,52). Briefly, we isolated PGCs from WT, $cKit^{V558\Delta/+}$ and $cKit^{V558\Delta/V558\Delta}$ embryos carrying *Oct4-ΔPE-EGFP* at E11.5 and cultured in DMEM/15% KSR (Invitrogen)/50 ng/ml bFGF (Sigma), 2000 U/ml LIF (EsGro)/60 ng/ml SCF (Invitrogen)/20 μM Forskolin (Sigma) and plated on Sl^{4}-m220 feeders. After 7–10 days, individual colonies were replated on STO feeders. EGC lines were maintained with STO cells in DMEM/15%KSR/LIF (1000 U/ml, EsGro).

Histology

Gonads collected from euthanized 14-week-old adults were weighed immediately. Testes were fixed in Bouin's solution overnight and ovaries were fixed in 10% neutral buffered formalin for 2 days before processing for paraffin embedding. Paraffin sections were cut serially at 5 μm and stained with hematoxylin and eosin.

Immunofluorescence staining and imaging

For whole-mount staining, embryos or gonads were fixed in methanol:dimethylsulfoxide (4:1) at −20°C, rehydrated and stained in PBS/2% non-fat milk/0.5% Tween with rocking as described (12). Cells were fixed in 4% PFA at room temperature and immunostained. Gonads were mounted on slides in Vectashield (Vector Labs), whereas whole embryos were cleared in methyl salicylate for imaging. Frozen sections were prepared from embryos fixed for 1 h in 4% PFA, embedded and cryosectioned in OCT and blocked with 5% goat serum in PBST (PBS/0.1% Triton X-100) before immunostaining. Primary antibodies used were as follows: SSEA1 (Developmental Studies Hybridoma Bank, 1:200), cleaved PARP (Cell Signaling 9544, 1:50), active caspase 3 (Promega G748A, 1:200), GCNA (a kind gift of George Enders, undiluted supernatant), P-JNK (Cell Signaling 9251, 1:50), P-AKT (Cell Signaling 4060, 1:200), P-ERK1/2 (Sigma

M9692, 1:100) and Stella (Abcam 19878, 1:200). Alexa-conjugated secondary antibodies were purchased from Invitrogen and used at 1:500. For EdU labeling, pregnant females were injected i.p. with 50 μg/g EdU (Invitrogen). Animals were euthanized after 4 h and embryos were fixed in 4% PFA and cryosectioned. EdU detection was carried out using the Click-iTTM EdU imaging kit (Invitrogen C10338). Imaging was carried out on an Olympus IX71 fluorescent microscope or on a Leica SP5 TCS microscope equipped with 405, 488, 543, 594 and 633 nm lasers. Confocal stacks were analyzed using Volocity (Improvision). The numbers of PGCs in whole-mount E10.5 embryos or E11.5 gonads were quantified as described elsewhere (12).

Flow cytometry

Oct4-ΔPE-GFP^{+} E11.5 gonad-mesonephri were dissociated in collagenase/dispase (5 mg/ml, Roche) and DNase I (1 mg/ml, Roche) for 10 min at 37°C, washed in staining medium (DMEM without phenol red + 2% FBS + 10 mM EDTA) with 1 μg/ml Sytox Blue viability stain (Invitrogen, S34857) and analyzed on a BD LSR II utilizing the 450/50 (Sytox Blue), 525/50 (GFP) and 660/20 (PE/Cy5) bandpass filters. For cKit surface staining, cells were stimulated with 60 ng/ml SCF for 20 min at 37°C, washed and stained with a cKit antibody conjugated to PE/Cy5 (clone 2B8, Abcam, ab81601) for 30 min on ice. EGCs were dissociated with 0.25% trypsin for 5 min at 37°C, and stained as above. Apoptosis was assessed by staining for extracellular phosphatidylserine, using annexin V–allophycocyanin (Invitrogen, A35110), according to the manufacturer's instructions. Sytox Blue was used to discriminate live cells (450/50), and APC was detected with the 660/20 bandpass filter. For proliferation assays, EGCs grown on STO feeder cells were pulsed for 1 h with BrdU (3 μg/ml), then trypsinized and fixed with 4% PFA for 15 min. After washing, antigen retrieval was performed with 2 M HCl for 20 min and neutralized with 0.1 M borate buffer (pH 8.5), permeabilized with 0.3% Triton-X-100 in PBS for 15 min at 25°C and stained with Alexa 594 conjugate-BrdU antibody (1:50, Invitrogen, 03–3940) and DAPI (4 μg/ml) for 30 min.

Expression studies

For gene expression studies, RNA was extracted using TRIzol or the RNeasy kit (Qiagen), reverse-transcribed using QScript cDNA SuperMix (Quanta Biosystems, 95048–100) and subjected to quantitative PCR for *cKit* at 50–100 cells/tube in SYBR Green using the following primers: CAGTCGTGCATTTCCTTTGAC and TTCCTCGCCTCCAAGAATTG. For western blotting, EGCs sorted from STO cells were starved in DMEM for 2 h and then stimulated with 50 ng/ml SCF for 10 min before lysis in RIPA buffer containing 1% NP-40, 0.25% deoxycholate acid, 150 mM NaCl, 0.1% SDS, 50 mM HEPES (pH 7.4), proteinase and phosphatase inhibitors (Roche). GISTs were isolated from three *cKit*$^{V558\Delta/+}$ male sibling mice at 12 weeks of age. Five micrograms of total protein was separated by SDS–PAGE and probed with the following antibodies (from Cell Signaling unless indicated): phospho JNK (9251, 1:1000), phospho AKT (4060, 1:1000), phospho-ERK1/2 (4370 1:2000), phospho-STAT3 (9145, 1:2000), AKT (4685, 1:1000), STAT3 (4904, 1:1000), ERK1/2 (4695, 1:1000), JNK (9258 1:1000), cKit (Santa Cruz, SC-168, 1:200), β-tubulin (LI-COR, 926–42211, 1:1000). The signals of western blotting were measured by the TotalLab Quant software.

Statistical analysis

Data were presented as the mean ± SEM of at least three separate experiments if not indicated in the figures. One-way ANOVA was used for comparison among more than two groups. Student's *t*-test was used for comparison between two groups. Values of $P < 0.05$ were accepted as significant.

SUPPLEMENTARY MATERIAL

Supplementary Material is available at *HMG* online.

ACKNOWLEDGEMENTS

The authors gratefully acknowledge P. Besmer and M. Bishop for providing mice, and K. Ebata and K. Blaschke for advice on EGC derivation. We thank K. Anderson, P. Besmer, R. Blelloch, M. Conti and the members of the Laird Lab for feedback.

Conflict of Interest statement. None declared.

FUNDING

This work was supported by the National Institutes of Health (1DP2OD007420 to D.J.L.), the Hellman Foundation, a pilot project under National Institute of Health (U54 HD055764), and California Institute of Regenerative Medicine Training Grant TB1-01194 to M.F.

REFERENCES

1. McLaren, A. (2003) Primordial germ cells in the mouse. *Dev. Biol.*, **262**, 1–15.
2. Tam, P.P. and Snow, M.H. (1981) Proliferation and migration of primordial germ cells during compensatory growth in mouse embryos. *J. Embryol. Exp. Morphol.*, **64**, 133–147.
3. Resnick, J.L., Bixler, L.S., Cheng, L. and Donovan, P.J. (1992) Long-term proliferation of mouse primordial germ cells in culture. *Nature*, **359**, 550–551.
4. Matsui, Y., Zsebo, K. and Hogan, B.L. (1992) Derivation of pluripotential embryonic stem cells from murine primordial germ cells in culture. *Cell*, **70**, 841–847.
5. Buehr, M., McLaren, A., Bartley, A. and Darling, S. (1993) Proliferation and migration of primordial germ cells in We/We mouse embryos. *Dev. Dyn.*, **198**, 182–189.
6. Mintz, B. and Russell, E.S. (1957) Gene-induced embryological modifications of primordial germ cells in the mouse. *J. Exp. Zool. Part A Ecol. Genet. Physiol.*, **134**, 207–237.
7. Runyan, C., Schaible, K., Molyneaux, K., Wang, Z., Levin, L. and Wylie, C. (2006) Steel factor controls midline cell death of primordial germ cells and is essential for their normal proliferation and migration. *Development*, **133**, 4861–4869.
8. Dolci, S., Williams, D.E., Ernst, M.K., Resnick, J.L., Brannan, C.I., Lock, L.F., Lyman, S.D., Boswell, H.S. and Donovan, P.J. (1991) Requirement for mast cell growth factor for primordial germ cell survival in culture. *Nature*, **352**, 809–811.

9. Godin, I., Deed, R., Cooke, J., Zsebo, K., Dexter, M. and Wylie, C.C. (1991) Effects of the steel gene product on mouse primordial germ cells in culture. *Nature*, **352**, 807–809.
10. Matsui, Y., Toksoz, D., Nishikawa, S., Williams, D., Zsebo, K. and Hogan, B.L. (1991) Effect of Steel factor and leukaemia inhibitory factor on murine primordial germ cells in culture. *Nature*, **353**, 750–752.
11. Farini, D., La Sala, G., Tedesco, M. and De Felici, M. (2007) Chemoattractant action and molecular signaling pathways of Kit ligand on mouse primordial germ cells. *Dev. Biol.*, **306**, 572–583.
12. Laird, D.J., Altshuler-Keylin, S., Kissner, M.D., Zhou, X. and Anderson, K.V. (2011) Ror2 enhances polarity and directional migration of primordial germ cells. *PLoS Genet.*, **7**, e1002428.
13. Kitayama, H., Kanakura, Y., Furitsu, T., Tsujimura, T., Oritani, K., Ikeda, H., Sugahara, H., Mitsui, H., Kanayama, Y., Kitamura, Y. *et al.* (1995) Constitutively activating mutations of c-kit receptor tyrosine kinase confer factor-independent growth and tumorigenicity of factor-dependent hematopoietic cell lines. *Blood*, **85**, 790–798.
14. Hirota, S., Isozaki, K., Moriyama, Y., Hashimoto, K., Nishida, T., Ishiguro, S., Kawano, K., Hanada, M., Kurata, A., Takeda, M. *et al.* (1998) Gain-of-function mutations of c-kit in human gastrointestinal stromal tumors. *Science*, **279**, 577–580.
15. Heaney, J.D., Lam, M.Y., Michelson, M.V. and Nadeau, J.H. (2008) Loss of the transmembrane but not the soluble kit ligand isoform increases testicular germ cell tumor susceptibility in mice. *Cancer Res.*, **68**, 5193–5197.
16. Sakuma, Y., Matsukuma, S., Yoshihara, M., Sakurai, S., Nishii, M., Kishida, T., Kubota, Y., Nagashima, Y., Inayama, Y., Sasaki, T. *et al.* (2008) Mutations of c-kit gene in bilateral testicular germ cell tumours in Japan. *Cancer Lett.*, **259**, 119–126.
17. Looijenga, L.H., de Leeuw, H., van Oorschot, M., van Gurp, R.J., Stoop, H., Gillis, A.J., de Gouveia Brazao, C.A., Weber, R.F., Kirkels, W.J., van Dijk, T. *et al.* (2003) Stem cell factor receptor (c-KIT) codon 816 mutations predict development of bilateral testicular germ-cell tumors. *Cancer Res.*, **63**, 7674–7678.
18. Sommer, G., Agosti, V., Ehlers, I., Rossi, F., Corbacioglu, S., Farkas, J., Moore, M., Manova, K., Antonescu, C.R. and Besmer, P. (2003) Gastrointestinal stromal tumors in a mouse model by targeted mutation of the Kit receptor tyrosine kinase. *Proc. Natl Acad. Sci. USA*, **100**, 6706–6711.
19. Nishida, T., Hirota, S., Taniguchi, M., Hashimoto, K., Isozaki, K., Nakamura, H., Kanakura, Y., Tanaka, T., Takabayashi, A., Matsuda, H. *et al.* (1998) Familial gastrointestinal stromal tumours with germline mutation of the KIT gene. *Nat. Genet.*, **19**, 323–324.
20. Roskoski, R. Jr (2005) Signaling by Kit protein-tyrosine kinase—the stem cell factor receptor. *Biochem. Biophys. Res. Commun.*, **337**, 1–13.
21. Duronio, V., Welham, M.J., Abraham, S., Dryden, P. and Schrader, J.W. (1992) p21ras activation via hemopoietin receptors and c-kit requires tyrosine kinase activity but not tyrosine phosphorylation of p21ras GTPase-activating protein. *Proc. Natl Acad. Sci. USA*, **89**, 1587–1591.
22. Serve, H., Hsu, Y.C. and Besmer, P. (1994) Tyrosine residue 719 of the c-kit receptor is essential for binding of the P85 subunit of phosphatidylinositol (PI) 3-kinase and for c-kit-associated PI 3-kinase activity in COS-1 cells. *J. Biol. Chem.*, **269**, 6026–6030.
23. Linnekin, D., Mou, S., Deberry, C.S., Weiler, S.R., Keller, J.R., Ruscetti, F.W. and Longo, D.L. (1997) Stem cell factor, the JAK-STAT pathway and signal transduction. *Leuk. Lymphoma*, **27**, 439–444.
24. Deberry, C., Mou, S. and Linnekin, D. (1997) Stat1 associates with c-kit and is activated in response to stem cell factor. *Biochem. J.*, **327**, 73–80.
25. Linnekin, D., DeBerry, C.S. and Mou, S. (1997) Lyn associates with the juxtamembrane region of c-Kit and is activated by stem cell factor in hematopoietic cell lines and normal progenitor cells. *J. Biol. Chem.*, **272**, 27450–27455.
26. Kissel, H., Timokhina, I., Hardy, M.P., Rothschild, G., Tajima, Y., Soares, V., Angeles, M., Whitlow, S.R., Manova, K. and Besmer, P. (2000) Point mutation in kit receptor tyrosine kinase reveals essential roles for kit signaling in spermatogenesis and oogenesis without affecting other kit responses. *EMBO J.*, **19**, 1312–1326.
27. Blume-Jensen, P., Jiang, G., Hyman, R., Lee, K.F., O'Gorman, S. and Hunter, T. (2000) Kit/stem cell factor receptor-induced activation of phosphatidylinositol 3′-kinase is essential for male fertility. *Nat. Genet.*, **24**, 157–162.
28. Kimura, Y., Jones, N., Kluppel, M., Hirashima, M., Tachibana, K., Cohn, J.B., Wrana, J.L., Pawson, T. and Bernstein, A. (2004) Targeted mutations of the juxtamembrane tyrosines in the Kit receptor tyrosine kinase selectively affect multiple cell lineages. *Proc. Natl Acad. Sci. USA*, **101**, 6015–6020.
29. Cook, M.S., Munger, S.C., Nadeau, J.H. and Capel, B. (2011) Regulation of male germ cell cycle arrest and differentiation by DND1 is modulated by genetic background. *Development*, **138**, 23–32.
30. Kurimoto, K., Yabuta, Y., Ohinata, Y., Shigeta, M., Yamanaka, K. and Saitou, M. (2008) Complex genome-wide transcription dynamics orchestrated by Blimp1 for the specification of the germ cell lineage in mice. *Genes Dev.*, **22**, 1617–1635.
31. Manova, K., Nocka, K., Besmer, P. and Bachvarova, R.F. (1990) Gonadal expression of c-kit encoded at the W locus of the mouse. *Development*, **110**, 1057–1069.
32. Gu, Y., Runyan, C., Shoemaker, A., Surani, A. and Wylie, C. (2009) Steel factor controls primordial germ cell survival and motility from the time of their specification in the allantois, and provides a continuous niche throughout their migration. *Development*, **136**, 1295–1303.
33. Garcia-Garcia, M.J., Eggenschwiler, J.T., Caspary, T., Alcorn, H.L., Wyler, M.R., Huangfu, D., Rakeman, A.S., Lee, J.D., Feinberg, E.H., Timmer, J.R. *et al.* (2005) Analysis of mouse embryonic patterning and morphogenesis by forward genetics. *Proc. Natl Acad. Sci. USA*, **102**, 5913–5919.
34. Nocka, K., Tan, J.C., Chiu, E., Chu, T.Y., Ray, P., Traktman, P. and Besmer, P. (1990) Molecular bases of dominant negative and loss of function mutations at the murine c-kit/white spotting locus: W37, Wv, W41 and W. *EMBO J.*, **9**, 1805–1813.
35. McCoshen, J.A. and McCallion, D.J. (1975) A study of the primordial germ cells during their migratory phase in Steel mutant mice. *Experientia*, **31**, 589–590.
36. Yoshimizu, T., Sugiyama, N., De Felice, M., Yeom, Y.I., Ohbo, K., Masuko, K., Obinata, M., Abe, K., Scholer, H.R. and Matsui, Y. (1999) Germline-specific expression of the Oct-4/green fluorescent protein (GFP) transgene in mice. *Dev. Growth Differ.*, **41**, 675–684.
37. Yee, N.S., Hsiau, C.W., Serve, H., Vosseller, K. and Besmer, P. (1994) Mechanism of down-regulation of c-kit receptor. Roles of receptor tyrosine kinase, phosphatidylinositol 3′-kinase, and protein kinase C. *J. Biol. Chem.*, **269**, 31991–31998.
38. Rossi, F., Ehlers, I., Agosti, V., Socci, N.D., Viale, A., Sommer, G., Yozgat, Y., Manova, K., Antonescu, C.R. and Besmer, P. (2006) Oncogenic Kit signaling and therapeutic intervention in a mouse model of gastrointestinal stromal tumor. *Proc. Natl Acad. Sci. USA*, **103**, 12843–12848.
39. Takeuchi, Y., Molyneaux, K., Runyan, C., Schaible, K. and Wylie, C. (2005) The roles of FGF signaling in germ cell migration in the mouse. *Development*, **132**, 5399–5409.
40. Timokhina, I., Kissel, H., Stella, G. and Besmer, P. (1998) Kit signaling through PI 3-kinase and Src kinase pathways: an essential role for Rac1 and JNK activation in mast cell proliferation. *EMBO J.*, **17**, 6250–6262.
41. Rossi, F., Yozgat, Y., de Stanchina, E., Veach, D., Clarkson, B., Manova, K., Giancotti, F.G., Antonescu, C.R. and Besmer, P. (2010) Imatinib upregulates compensatory integrin signaling in a mouse model of gastrointestinal stromal tumor and is more effective when combined with dasatinib. *Mol. Cancer Res.*, **8**, 1271–1283.
42. Kwon, J.G., Hwang, S.J., Hennig, G.W., Bayguinov, Y., McCann, C., Chen, H., Rossi, F., Besmer, P., Sanders, K.M. and Ward, S.M. (2009) Changes in the structure and function of ICC networks in ICC hyperplasia and gastrointestinal stromal tumors. *Gastroenterology*, **136**, 630–639.
43. Hong, L., Munugalavadla, V. and Kapur, R. (2004) c-Kit-mediated overlapping and unique functional and biochemical outcomes via diverse signaling pathways. *Mol. Cell. Biol.*, **24**, 1401–1410.
44. Chi, P., Chen, Y., Zhang, L., Guo, X., Wongvipat, J., Shamu, T., Fletcher, J.A., Dewell, S., Maki, R.G., Zheng, D. *et al.* (2010) ETV1 is a lineage survival factor that cooperates with KIT in gastrointestinal stromal tumours. *Nature*, **467**, 849–853.
45. Bauer, S., Duensing, A., Demetri, G.D. and Fletcher, J.A. (2007) KIT oncogenic signaling mechanisms in imatinib-resistant gastrointestinal stromal tumor: PI3-kinase/AKT is a crucial survival pathway. *Oncogene*, **26**, 7560–7568.
46. La Sala, G., Farini, D. and De Felici, M. (2009) Proapoptotic effects of lindane on mouse primordial germ cells. *Toxicol. Sci.*, **108**, 445–451.
47. Kimura, T., Tomooka, M., Yamano, N., Murayama, K., Matoba, S., Umehara, H., Kanai, Y. and Nakano, T. (2008) AKT signaling promotes

derivation of embryonic germ cells from primordial germ cells. *Development*, **135**, 869–879.
48. De Miguel, M.P., Cheng, L., Holland, E.C., Federspiel, M.J. and Donovan, P.J. (2002) Dissection of the c-Kit signaling pathway in mouse primordial germ cells by retroviral-mediated gene transfer. *Proc. Natl Acad. Sci. USA*, **99**, 10458–10463.
49. Kimura, T., Suzuki, A., Fujita, Y., Yomogida, K., Lomeli, H., Asada, N., Ikeuchi, M., Nagy, A., Mak, T.W. and Nakano, T. (2003) Conditional loss of PTEN leads to testicular teratoma and enhances embryonic germ cell production. *Development*, **130**, 1691–1700.
50. Bauer, S., Yu, L.K., Demetri, G.D. and Fletcher, J.A. (2006) Heat shock protein 90 inhibition in imatinib-resistant gastrointestinal stromal tumor. *Cancer Res.*, **66**, 9153–9161.
51. Xiang, Z., Kreisel, F., Cain, J., Colson, A. and Tomasson, M.H. (2007) Neoplasia driven by mutant c-KIT is mediated by intracellular, not plasma membrane, receptor signaling. *Mol. Cell. Biol.*, **27**, 267–282.
52. Leitch, H.G., Blair, K., Mansfield, W., Ayetey, H., Humphreys, P., Nichols, J., Surani, M.A. and Smith, A. (2010) Embryonic germ cells from mice and rats exhibit properties consistent with a generic pluripotent ground state. *Development*, **137**, 2279–2287.
53. Lin, A. (2003) Activation of the JNK signaling pathway: breaking the brake on apoptosis. *Bioessays*, **25**, 17–24.
54. Logan, S.K., Falasca, M., Hu, P. and Schlessinger, J. (1997) Phosphatidylinositol 3-kinase mediates epidermal growth factor-induced activation of the c-Jun N-terminal kinase signaling pathway. *Mol. Cell. Biol.*, **17**, 5784–5790.
55. Weston, C.R., Wong, A., Hall, J.P., Goad, M.E., Flavell, R.A. and Davis, R.J. (2004) The c-Jun NH2-terminal kinase is essential for epidermal growth factor expression during epidermal morphogenesis. *Proc. Natl Acad. Sci. USA*, **101**, 14114–14119.
56. Yu, C., Minemoto, Y., Zhang, J., Liu, J., Tang, F., Bui, T.N., Xiang, J. and Lin, A. (2004) JNK suppresses apoptosis via phosphorylation of the proapoptotic Bcl-2 family protein BAD. *Mol. Cell*, **13**, 329–340.
57. Tiwari, V.K., Stadler, M.B., Wirbelauer, C., Paro, R., Schubeler, D. and Beisel, C. (2011) A chromatin-modifying function of JNK during stem cell differentiation. *Nat. Genet.*, **44**, 94–100.
58. Duensing, A., Medeiros, F., McConarty, B., Joseph, N.E., Panigrahy, D., Singer, S., Fletcher, C.D., Demetri, G.D. and Fletcher, J.A. (2004) Mechanisms of oncogenic KIT signal transduction in primary gastrointestinal stromal tumors (GISTs). *Oncogene*, **23**, 3999–4006.
59. Szabo, P.E., Hubner, K., Scholer, H. and Mann, J.R. (2002) Allele-specific expression of imprinted genes in mouse migratory primordial germ cells. *Mech. Dev.*, **115**, 157–160.
60. Yamaguchi, T.P., Bradley, A., McMahon, A.P. and Jones, S. (1999) A Wnt5a pathway underlies outgrowth of multiple structures in the vertebrate embryo. *Development*, **126**, 1211–1223.
61. Anderson, R., Copeland, T.K., Scholer, H., Heasman, J. and Wylie, C. (2000) The onset of germ cell migration in the mouse embryo. *Mech. Dev.*, **91**, 61–68.